analytical chemistry

Article

pubs.acs.org/ac

Accelerated Immunoassays Based on Magnetic Particle Dynamics in a Rotating Capillary Tube with Stationary Magnetic Field

Jun-Tae Lee, L. Sudheendra, and Ian M. Kennedy*

Department of Mechanical and Aerospace Engineering, University of California Davis, California 95616, United States

ABSTRACT: A rapid and simple magnetic particle-based immunoassay has been demonstrated in a capillary mixing system. Antibody-coated micrometer size superparamagnetic polystyrene (SPP) particles were used in an assay for rabbit IgG in a sandwich (noncompetitive) format. The kinetics of the assay was compared between a plate-based system and a single capillary tube. The interaction between the antigen (R-IgG) and the antibody (anti-R-IgG) that was carried by the SPP particles in a rotating capillary was tested under a stationary magnetic field. Competing magnetic and viscous drag forces helped to enhance the interaction between the analyte and the capture antibodies on the particles. The dimensionless Mason number (Mn) was employed to characterize the magnetic particle dynamics; a previously determined critical Mason number (Mn_c) was employed as a guide to the appropriate experimental conditions of magnetic field strength and rotational speed of the capillary. The advantage of the rotating capillary system included a short assay time and a reduced reactive volume (20 μL). The results show that the immunoassay kinetics were improved by the formation of chains of the SPP particles for the conditions that corresponded to the critical Mason number.

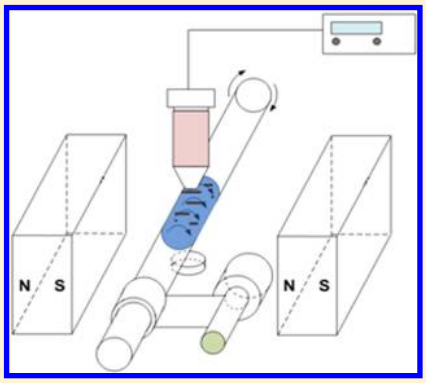

An immunoassay is a highly sensitive detection method that uses the specific interactions between antigens (the analytes) and their corresponding antibodies. It is popularly used to analyze biomolecular interactions in a 96-well plate in the conventional format. The enzyme-linked immunosorbent assay (ELISA) is one example of this format. A large effort has been expended over the years to speed up the conventional immunoassay. For example, flow-based assays have been developed to improve the rate of binding between capture and antibodies and target.[1] Miniaturization of the format has also played a key role in improving assay handling, in providing desktop automation, reduced costs, faster assay times, and increased sensitivity.[2] Microfluidic systems have been commonly adopted in biological assays,[3] immunoassays,[4] and DNA separation and analysis,[5] as well as environmental monitoring[6] due to their rapid assay time, reduced reagent consumption, integrated multiple assay steps, and cost effectiveness.[7] A microchip has also been employed in immunoassay to improve the microfluidic system to reduce analysis time.[8]

Magnetic particles (MPs) have been applied to develop fast and miniaturized bioassays because nano/microparticles offer a high surface to volume ratio and enhanced fluid-phase kinetics for biomolecular binding.[9] The magnetic properties of the MPs enable fast and easy magnetic separation of captured analyte. In addition, MPs can be easily manipulated using magnetic fields to generate effective mixing[10] and requiring a smaller amount of antibody[11] with sensitive detection.[12] MPs were demonstrated as micro- and nanomixers in microfluidic systems.[13] Mixing and rapid analysis of fluids are important challenges in current microfluidic systems because the interaction between reagents in the fluid is limited by the laminar flow and small diffusivities[14] of relatively large biomolecules.

MPs in a rotating magnetic field have been studied by several groups to improve mixing. Magnetic particle chain formation was used for accelerated transport in fluids.[15] Kang et al.[16] studied chaotic mixing induced by chains of magnetic particle. Superparamagnetic polystyrene (SPP) particle chains were demonstrated to enhance mixing in small liquid volumes under a rotating magnetic field.[12] However, rotating magnetic fields that are created by electromagnets can lead to undesirable heat generation; biological reactions are sensitive to temperature changes that can confound the measurement. The system is bulky and offers limited optical access. In order to avoid some of the undesirable aspects of a rotating magnetic field, we have explored the inverse system: a rotating capillary tube in a stationary magnetic field.

Initially, SPP particles are uniformly dispersed single particles; once SPP particles are exposed to an external magnetic field, SPP particles acquire magnetic dipole moments (m) to form chains and align with the field direction.

$$m = \frac{4}{3}\pi a^3 \mu_o \chi \mathbf{H_o}$$

Here, a is the particle radius, χ is the particle susceptibility, μ_o is the magnetic permeability of vacuum, and $\mathbf{H_o}$ is an external magnetic field of magnitude. A dimensionless Mason number, the ratio of viscous force to magnetic force, can be used to

Received: July 3, 2012
Accepted: August 30, 2012
Published: August 30, 2012

   dx.doi.org/10.1021/ac301848q | *Anal. Chem.* 2012, 84, 8317–8322

characterize the magnetic particle dynamics in a rotating magnetic field.[16,17] The Mason number can similarly be used to characterize the dynamics of SPP particles and the mixing effect in a rotating capillary system.[18] In this study, we define our dimensionless Mason number (Mn) similar to Biswal and Gast[19] as

$$\mathrm{Mn} = \frac{32\eta\omega}{\mu_o \chi^2 \mathbf{H_o}^2}$$

where η is the viscosity of the fluid, ω is the angular velocity of the capillary tube, μ_0 is the magnetic permeability of vacuum, χ is the particle susceptibility, and $\mathbf{H_o}$ is the external magnetic field strength. At a higher Mn, viscous forces are dominant; therefore, particle chains starts to break-up.[20] Previously, we established a critical Mn ($\mathrm{Mn_c}$ = 0.012) for a stationary magnetic field with a rotating capillary tube.

This paper explores the speed advantage of mixing in a stationary magnetic field and rotating capillary tube by studying the kinetics of an immunoassay using antibodies immobilized on the surfaces of SPP particles; the sensitivity and limit of detection were not the focus of this study. By rotating the capillary, the particle−liquid interaction is enhanced with increased mixing efficiency and molecular binding rates. In addition, the rotation of the capillary can be stopped to hold the magnetic particles against the tube wall while washing proceeds, followed by resumed rotation of the capillary for the following steps of the assay, leading to a simple, easily controlled format for bioassays. The mixing effect is demonstrated in the present work by application of an immunoassay at different Mason numbers.

EXPERIMENTAL SECTION

Materials and Reagents. The SPP particles (Dynabeads M-280, 10 mg/mL, Carlsbad, CA) were coated with purified sheep antirabbit IgG primary antibodies. Rabbit IgG was used as the antigen, and antirabbit IgG−horseradish peroxidase (HRP) conjugate was used as the secondary antibody. The mean particle diameter was d = 2.8 μm, density ρ = 1400 kg/m^3, and the particle susceptibility χ = 0.756. Tween 20 and bovine serum albumin (BSA) were obtained from Sigma-Aldrich (St. Louis, MO); biotin was obtained from Thermo Fisher Scientific (Rockford, IL). Phosphate buffer saline (PBS) (pH = 7.5) was 1 mM phosphate buffer saline. PBST is PBS with 0.05% Tween 20 (v/v). The particle surface was blocked with 1 mL of 3% BSA/PBS for 1 h in a rotating mill.

IMMUNOASSAY

Magnetic Particle-Based Immunoassay in a 96-Well Plate. The rabbit IgG assay was run in a 96-well plate as a point of comparison with our rotating capillary scheme. The SPP particle-based sandwich ELISA was performed with a particle concentration of 0.06% wt.[18] Nunc Maxisorp 96-well plates (Nunc-immuno plate, Roskilde, Denmark) were blocked with 3% BSA/PBS. The stock (10 mg/mL in PBS/BSA) solution of rabbit IgG, derived from goats (diluted to 50 pg/mL−50 μg/mL), was used for determining the standard curve. To each sample well, 50 μL of magnetic particles and 50 μL of rabbit IgG of predetermined concentrations were added, and the mixture was incubated at room temperature for 1 h on a plate orbital shaker. Nonspecifically bound secondary antibodies were removed by applying a magnetic field to isolate the particles followed by washing with PBST (PBS plus 0.05% Tween 20) three times. Then, 100 μL of antirabbit IgG−horseradish peroxidase (HRP) conjugate (Sigma, St.Louis, MO) was added to each well, and the solution was incubated for 1 h on a plate orbital shaker. A colorless HRP substrate buffer was prepared by adding 400 μL of 0.6% TMB (tetramethylbenzidine) in dimethyl sulfoxide (DMSO) and 100 μL of 1% hydrogen peroxide (H_2O_2) to 25 mL of citrate−acetate buffer. This HRP substrate buffer was added and incubated for 15 min, and the solution turned blue. The intensity of the color was proportional to the concentration the rabbit IgG. Finally, 50 μL of 2 M H_2SO_4 was added as a stop solution to change the color to a stable yellow. ELISA absorbances at 450 nm were measured with a Spectramax M2 plate reader (Molecular Devices, Menlo Park, CA). Samples were run in triplicates.

Rotating Capillary Tube Immunoassay. A simple rotating capillary system in a constant magnetic field was designed for a fast immunoassay. A disposable borosilicate capillary tube (outside radius = 4 mm, inside radius (r_c) = 2.3 mm) was used in all the experiments. Two permanent rectangular (50.8 mm long; 12.7 mm wide and 3.17 mm thick) neodymium−iron−boron magnets (Magcraft, Vienna, VA) were placed symmetrically on either side of capillary tube, such that the axis perpendicular to the largest area of the magnet and the corresponding magnetic field was perpendicular to the axis of the capillary tube. The capillary tube was attached to an electrically controlled motor (Tamiya, Japan). The schematic experimental setup is shown in Figure 1. The

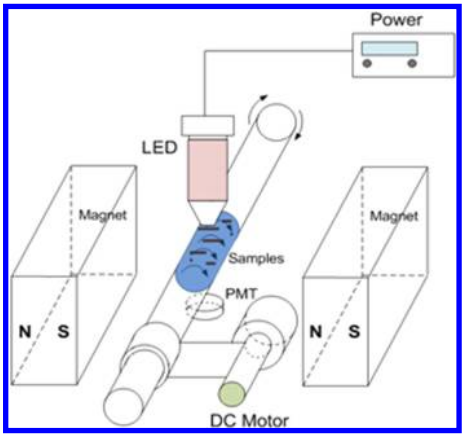

Figure 1. Schematic illustration of the experimental setup.

strength of the magnetic field was controlled by changing the distance between the two magnets; the maximum magnetic field of 300 mT was measured with a Gauss meter (Transcat, NY). The uniformity of the magnetic field (3.4−300 mT) was confirmed both experimentally and numerically (Vizimag 3.193) (Figure 2).

The capillary tube was rinsed with PEG (polyethylene glycol) solution to prevent adhesion of the particles onto the inner wall of the tube. The SPP particles were diluted to 0.06% wt in 1 mM PBS (Phosphate buffered saline) solution; a volume of 20 μL of suspension was used in all experiments. The particles were freely suspended in buffer solution in the absence of a magnetic field. The application of a uniform magnetic field induced the formation of chains of particles. For the rotation experiments, the capillary tube was subjected to a steady rotation with angular velocities, ω, between 0.73 and 0.80 rad·s^{-1}. The initial condition for all experiments consisted of

dx.doi.org/10.1021/ac301848q | Anal. Chem. 2012, 84, 8317−8322

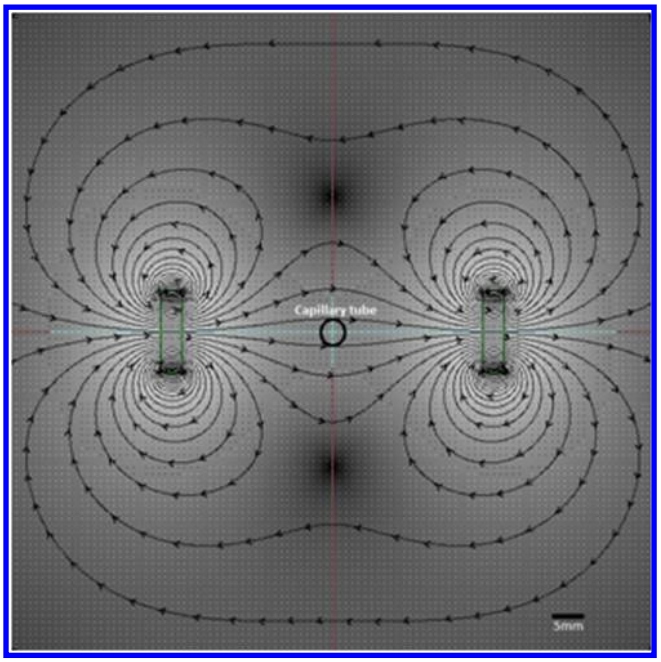

Figure 2. Magnetic fields were simulated with Vizimag software (Vizimag 3.193). Neodymium−iron−boron permanent magnets with 12.7 mm height and 3.17 mm width from Magcraft, Vienna, VA were located 50 mm apart. The capillary is at the center of the magnets.

uniformly dispersed single particles. The magnetic field and rotation of the capillary tube were then applied to test the immunoassay performance. The time dependence (kinetics) of the incubation conditions was investigated to understand the mixing efficiency. When the analyte is added, the magnetic field and rotation of capillary were applied simultaneously at $t = 0$.

The immunoassay for rabbit IgG was carried out with 0.06% wt/v in PBS buffer solution. Kinetics experiments were carried out with constant rabbit IgG concentration (50 pg/mL) in 40 μL volume. This concentration was chosen for all of the capillary work because it is at the limit of detection that we determined the 96-well plate ELISA. A simple protocol was followed to run an experiment: a micropipet was used to introduce the SPP particle solution into the open capillary tube, followed by the analyte solution for the first incubation; a secondary antibody−HRP conjugate (40 μL) was then pipetted into the capillary for the second incubation step. After the first incubation, the binding of antigen with the primary antibody, the SPP particles were held on one side of the stationary capillary tube by the external magnet while the remaining solution was washed with PBST to remove unbound antigen, in a similar manner to that used with magnetic particles in a 96-well plate. Then, particles were redispersed in buffer solution−PBS (20 μL) with rotation of the capillary prior to the second incubation step.

The binding of antigen and the primary antibody was investigated for different Mns. The Mn was changed by changing the rotation speeds and external magnetic fields. The IgG was quantified by detecting the light absorption of the solution. The absorptivities were measured and analyzed for different incubation times from 5 to 80 min. The light absorption was proportional to the amount of rabbit IgG concentration since the HRP was conjugated to the secondary antibody.

The schematic diagram of the sandwich immunoassay experiment is shown in Figure 3. For quantification of the

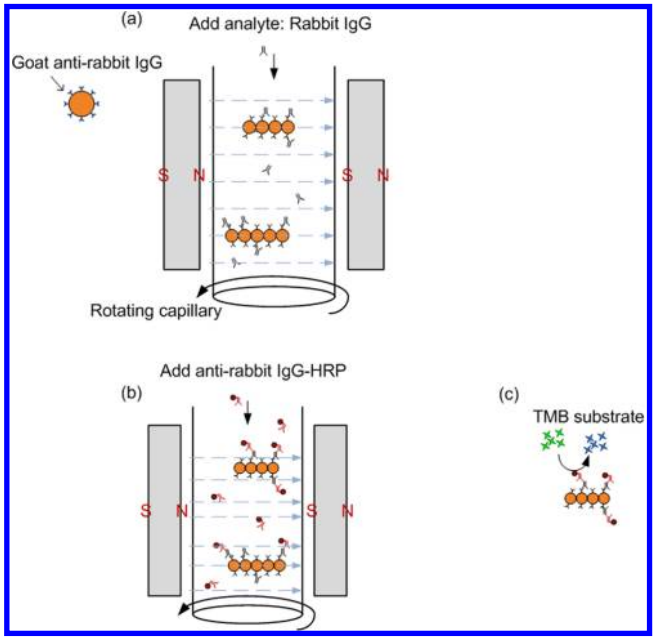

Figure 3. Schematic illustration of sandwich ELISA based on superparamagnetic particles in the rotating capillary: (a) antirabbit IgG antibody-coated magnetic particles in liquid suspension initially formed chains in stationary magnetic fields; then, the capillary was rotated with an angular frequency ω; first incubation step with target antibody (rabbit IgG); target antigen binds to particles; (b) during a second incubation, the antirabbit IgG conjugated with HRP enzyme was bound to immunocomplex; (c) TMB substrate was added to the assay to develop color, producing signal proportional to the amount of target concentration in the sample.

rabbit IgG, a white light-emitting diode (LED) source was focused on the 40 μL volume in the capillary using a cylindrical lens (Thorlabs, NJ) such that the volume of the solution was completely exposed to the light. The absorption from the particle complex was measured by focusing the transmitted light on the opposite side of the capillary tube onto the PMT (Photomultiplier tube, H10721, Hamamatsu, Japan) detection system. The current output from the PMT was measured by a Pico-ampere meter (Keithley, OH). The obtained signal intensities were normalized against the maximum signal intensity at $t = 0$. A laboratory DC power supply (GPS-3030D, GW, Taiwan) was used to power the LED and the PMT. Conditions for the plate-based and for the capillary-based experiments are presented in Table 1.

RESULTS AND DISCUSSION

The 0.06% concentration of SPP particles was held constant with different volumes in a microtiter 96-well plate to generate

Table 1. Comparison of Parameters Used for 96-Well Plate and Capillary

	first incubation time, min	second incubation time, min	volume, μL
96-well plate	60	60	100
capillary system (obtained a detectable signal)	10−30	10−30	40

dx.doi.org/10.1021/ac301848q | *Anal. Chem.* 2012, 84, 8317−8322

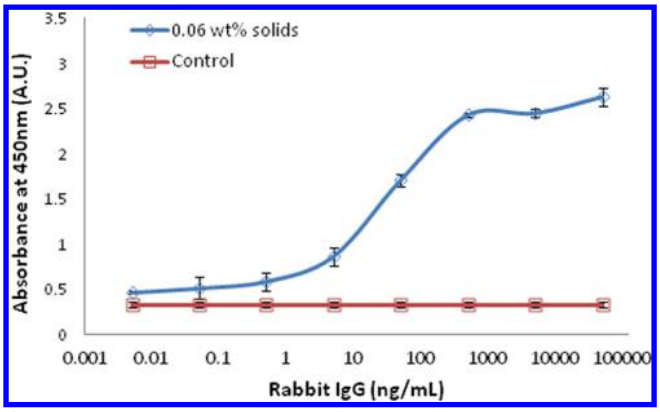

Figure 4. Standard curve of rabbit IgG concentration in ELISA (incubation time = 60 min) with magnetic particles in a 96-well plate. The signal and error bars represent averages based on three measurements.

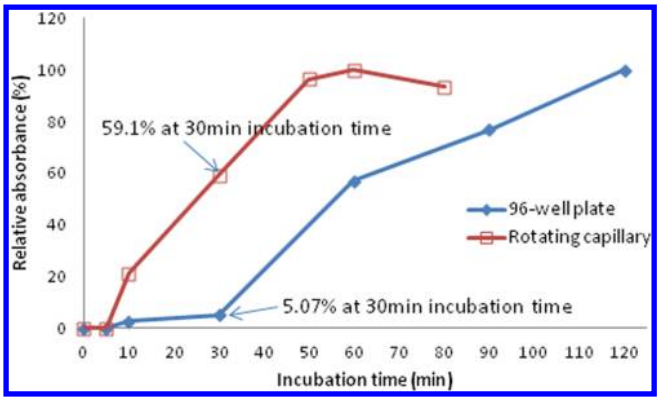

Figure 6. The relative signal for an ELISA in a 96-well plate was compared as a function of time with the signal from the rotating capillary (Mn ~ 0.01) (Magnetic particle diameter, d_p = 2.8 μm, 0.06 wt % solids, R-IgG = 50 pg/mL).

a standard immunoassay curve with a plate reader (Figure 4). The curve was used to determine the limit of detection of the assay in this format; the concentration of analyte at the limit of detection was used for subsequent comparison of the kinetics of this assay in the capillary-based assay. Although 100 μL was the minimum volume required to generate data from the microtiter plate, 40 μL was sufficient to perform the experiment in the capillary tube. The SPP particle concentration of 0.06% was chosen as it was established to be a good concentration for mixing in our previous studies.[18] As a negative control, we used only secondary antibody−HRP conjugates without analyte; the control in all cases showed negligible nonspecific interactions. From Figure 4, the limit of detection for the detection of rabbit IgG was established to be about 50 pg/mL, based on the lower end of the linear range of detection. This concentration was three times the standard deviation of the negative control. We used the concentration of IgG at the limit of detection for the subsequent measurements in the rotating capillary system.

Effect of Rotation and Magnetic Field on the Binding Kinetics in a Capillary Tube. The antirabbit IgG coated MPs were tested in the rabbit IgG assay with capillary rotation at a concentration that conforms with the limit of detection found in the 96-well plate ELISA. Our focus here is simply on comparing the kinetics of the assays so all the capillary measurements were performed at this concentration of analyte, although a standard curve could be generated by using different analyte concentrations. Measurements of absorbance are indicative of analyte concentration. The absorbance data shown in Figure 5, after the reaction is complete at about 1 h, indicate that the standard deviation (based on triplicate measurements) is relatively small. The sensitivity of the capillary system is at least as good as the 96-well format.

Our focus is on the impact of the motion of the magnetic particles on the speed of the assay. The interaction of magnetic particles is strongly dependent on the distance ($F_{interaction} \propto 1/r^4$) between particles and depends on particle concentrations.[19] In the capillary rotation experiment, the particles interact with each other in the suspension; their assembly into long chains is governed by competing viscous forces and magnetic forces. Owing to the low Reynolds number, the primary antibody-

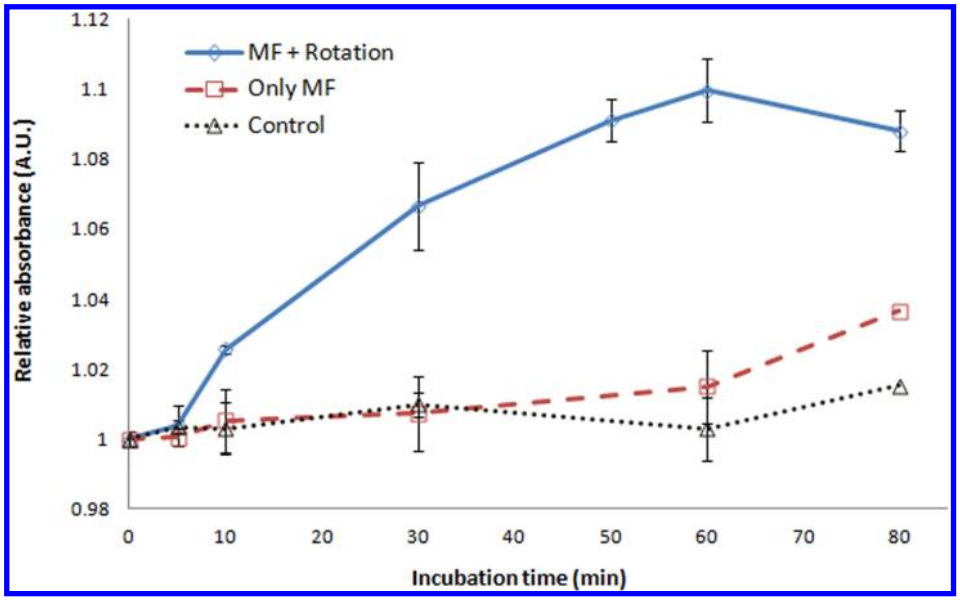

Figure 5. The signal intensities with MPs binding rabbit IgG and antirabbit IgG conjugated HRP, with and without rotation of the capillary. The signal intensities were normalized against the maximum signal intensity at t = 0.

dx.doi.org/10.1021/ac301848q | Anal. Chem. 2012, 84, 8317−8322

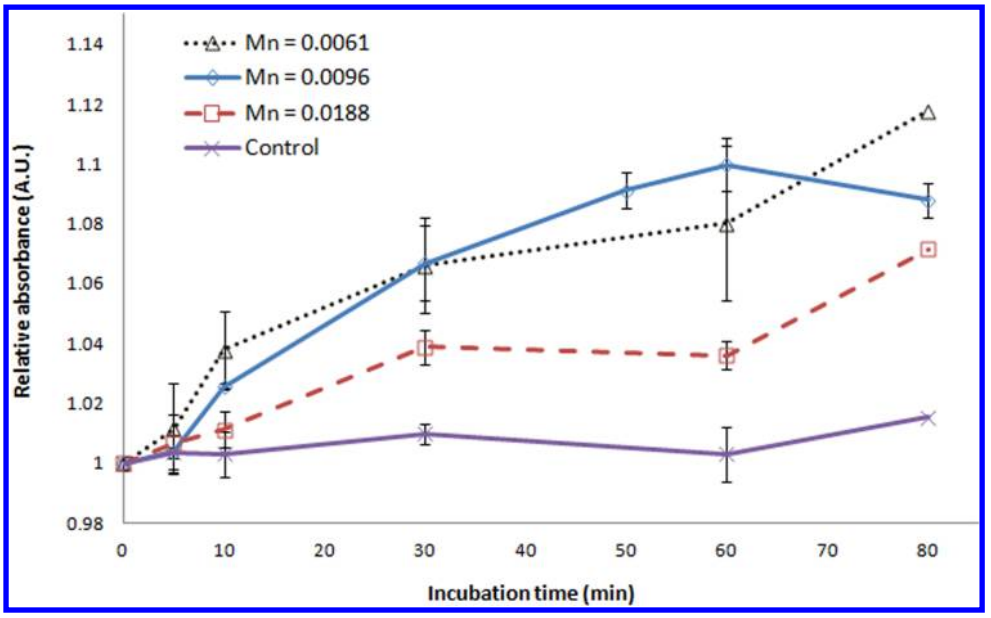

Figure 7. The relative signal intensity reflects the difference in the binding kinetics for different Mason numbers (Magnetic particle diameter, d_p = 2.8 μm, 0.06 wt % solids; R-IgG = 50 pg/mL).

Table 2. Mason Numbers for Different Conditions

	M_n = 0.0061	M_n = 0.0096	M_n = 0.0188
magnetic field ($\mathbf{H}_o$), mT	7.45	5.56	4.24
angular velocity (ω), rad/s	0.804	0.735	0.804

coated magnetic particles would require a long time to capture analytes, even in a small volume. The ratio of the viscous and magnetic forces can be tuned (as described by the Mn) to achieve enhanced mixing when the binding is diffusion limited. Figure 5 shows the difference in the binding kinetics for the conditions where the tube is rotating and where it is stationary. The binding between antibodies and antigen is considerably enhanced when the capillary tube is rotated in the stationary magnetic field. From our previous results, we expect that chains of magnetic particles will form at this value of Mn without the formation of dense aggregates. Single particles in suspension offer little assistance in mixing because they follow the fluid with great fidelity. On the other hand, chains undergo a rotation in the fluid, sweeping out a volume of the fluid and intercepting free analyte in solution. This is the condition that we aim for in order to enhance mixing and reaction without the loss of active binding sites that occurs when particles aggregate into lumps.

Comparison of Assay Kinetics in a 96-Well Plate and in the Rotating Capillary. The kinetic of a magnetic particle-based ELISA assay in a 96-well plate was examined by collecting a time course of the assay. Generally, the antigen–antibody interaction is a very fast biomolecular reaction. The antigen–antibody interaction as a biomolecular reaction can be described by:

$$A + B \underset{k_{-o}}{\overset{k_o}{\rightleftharpoons}} AB$$

where AB is the antibody–antigen complex, A is the antigen, B is antibody, k_o is the reaction on-rate constant, and k_{-o} is the reverse rate constant. The antibody reaction rate (k_o) is in the range of 10^5–10^6 M^{-1} s^{-1}. The reverse reaction rate (k_{-o}) is very low, and the reaction can therefore be regarded as quasi-irreversible.[21] The ratio between the chemical reaction rate and the relative rates of diffusion is described by the Damköhler number, Da. A small Damköhler number signifies that the chemical reaction is slow compared to the rate of diffusion. A large Damköhler number indicates that the chemical reaction is fast compared to the rate of diffusion and the reaction is limited by diffusion. Applying the antibody reaction rate and the diffusion coefficient of an antibody (a representative value for an IgG antibody or protein antigen is 4×10^{-11} m^2s^{-121}), the Damköhler number was about 7×10^5 for the rotating capillary system. Thus, the magnetic particle-based ELISA is limited by diffusion. Butler[22] observed that diffusion has a strong effect on the assay kinetics in the microtiter plate immunoassays based on microparticles; the immunoreaction reached equilibrium after 60–300 min of incubation time.[23] We would expect, therefore, that an improvement in mixing should enhance the kinetics of the assay.

The immunoassay assay kinetics was indeed improved by running the assay in the rotating capillary within a stationary magnetic field (Figure 6). The light absorption due to the formation of the IgG–IgG complex in the rotating capillary reached equilibrium faster than in a conventional 96-well plate analysis due to the improved interaction between the fluid and the rotating magnetic chains that carried the primary antibody. At an incubation time of 30 min, the relative signal intensity was enhanced by over a factor of 11. A detectable signal was obtained within 10 min of incubation time in the capillary experiment.

In order to clearly determine the impact of mixing on the kinetics of the immunoassay, the assay was run at three Mason numbers (Mn), ranging from 6.1×10^{-3} to 1.9×10^{-2}. The results are shown in Figure 7, and conditions for the three Mason numbers are presented in Table 2. The interaction of magnetic particles with analyte reached equilibrium faster (after 50 min) when the Mn was close to the critical Mn_c = 0.012. Above this critical value of Mn, the kinetics of the immunoassay was negatively impacted. When the Mn is increased above the critical value, chain length decreases due to the increased disruptive impact of viscous drag on particle chains relative to

dx.doi.org/10.1021/ac301848q | Anal. Chem. 2012, 84, 8317–8322

the interparticle magnetic forces that keep chains intact. We have previously measured average chain lengths using video microscopy (data not shown) and found that particle chains begin to break at the Mn_c = 0.012. At high Mn, viscous forces dominate chain formation and the particles exist as single entities that follow the fluid exactly, with no effect on mixing. At a lower Mn, particles form chains in the magnetic field. The particle chains do not follow the fluid but rather they sweep out a volume of fluid as they rotate to maintain their alignment with the external magnetic field. The sweeping action reduces the limitation of diffusion and improves the interaction between antibodies on the particles and the analytes in solution. If the Mn is reduced too much, particle chains will collapse into aggregates that lose surface area and available binding sites. The results suggest that it is possible to find an optimum Mn that supports enhanced assay kinetics with magnetic particles.

■ CONCLUSIONS

A sandwich enzyme-linked immunosorbent assay, with capture antibodies attached to magnetic beads, was evaluated in a rotating capillary subjected to a constant external magnetic field with varying rotation speeds and hence varying Mason numbers (Mn). The rotating capillary system improved the performance of the assay by reducing the reaction volume (by 2.5 times) and by decreasing the time for relative signals saturation by 10−30 min. A detectable signal due to the immuno-complex formation was observed as early as 10 min into the incubation period. The rate of the mixing-limited immunoreaction was significantly influenced by the Mason number. The results indicated that a critical Mason number (Mn_c) for chain formation is the lowest Mn at which the immunoreaction kinetics can be improved; the assay kinetics can be improved by selecting a Mn that results in chain formation. Our results showed the relative motion of particle chains in the fluid served to overcome the limitation of diffusion on the interaction between antibodies and analytes.

■ AUTHOR INFORMATION

Corresponding Author

*Phone: 530-752-2796. Fax: 530-752-4158. E-mail: imkennedy@ucdavis.edu.

Notes

The authors declare no competing financial interest.

■ ACKNOWLEDGMENTS

The project described was supported by Award Number P42ES004699 from the National Institute of Environmental Health Sciences. The content is solely the responsibility of the authors and does not necessarily represent the official views of the National Institute of Environmental Health Sciences or the National Institutes of Health. The project was also supported by the National Research Initiative of the USDA Cooperative State Research, Education and Extension Service, grant number 2009-35603-05070. This work was also supported by grant 200911634 from NIAID, NIH.

■ REFERENCES

(1) Hartwell, S. K.; Grudpan, K. *Microchim. Acta* **2010**, *169*, 201−220.
(2) Ekins, R. *Nucl. Med. Biol.* **1994**, *21*, 495−521.
(3) Adamo, A.; Jensen, K. F. *Lab Chip* **2008**, *8*, 1258−1261.
(4) (a) Luo, Y. Q.; Yu, F.; Zare, R. N. *Lab Chip* **2008**, *8*, 694−700. (b) Noroozi, Z.; Kido, H.; Peytavi, R.; Nakajima-Sasaki, R.; Jasinskas, A.; Micic, M.; Felgner, P. L.; Madou, M. J. *Rev. Sci. Instrum.* **2011**, *82*, 064303.
(5) (a) Chung, Y. C.; Lin, Y. C.; Chueh, C. D.; Ye, C. Y.; Lai, L. W.; Zhao, Q. *Electrophoresis* **2008**, *29*, 1859−1865. (b) Yoon, T. H.; Hong, L. Y.; Lee, C. S.; Kim, D. P. *J. Phys. Chem. Solids* **2008**, *69*, 1325−1329. (c) Hopwood, A. J.; Hurth, C.; Yang, J. N.; Cai, Z.; Moran, N.; Lee-Edghill, J. G.; Nordquist, A.; Lenigk, R.; Estes, M. D.; Haley, J. P.; McAlister, C. R.; Chen, X.; Brooks, C.; Smith, S.; Elliott, K.; Koumi, P.; Zenhausern, F.; Tully, G. *Anal. Chem.* **2010**, *82*, 6991−6999.
(6) (a) Blankenstein, G.; Larsen, U. D. *Biosens. Bioelectron.* **1998**, *13*, 427−438. (b) Baeumner, A. J. *Anal. Bioanal. Chem.* **2003**, *377*, 434−445.
(7) (a) He, B.; Burke, B. J.; Zhang, X.; Zhang, R.; Regnier, F. E. *Anal. Chem.* **2001**, *73*, 1942−1947. (b) Park, S. J.; Kim, J. K.; Park, J.; Chung, S.; Chung, C.; Chang, J. K. *J. Micromech. Microeng.* **2004**, *14*, 6−14.
(8) (a) Teste, B.; Malloggi, F.; Siaugue, J. M.; Varenne, A.; Kanoufi, F.; Descroix, S. *Lab Chip* **2011**, *11*, 4207−4213. (b) Yatsushiro, S.; Akamine, R.; Yamamura, S.; Hino, M.; Kajimoto, K.; Abe, K.; Abe, H.; Kido, J.; Tanaka, M.; Shinohara, Y.; Baba, Y.; Ooie, T.; Kataoka, M. *Plos One* **2011**, *6*, No. e18807.
(9) (a) Munir, A.; Wang, J.; Zhou, H. S. *IET Nanobiotechnol.* **2009**, *3*, 55−64. (b) Kim, K. S.; Park, J. K. *Lab Chip* **2005**, *5*, 657−664.
(10) (a) Dosev, D.; Nichkova, M.; Dumas, R. K.; Gee, S. J.; Hammock, B. D.; Liu, K.; Kennedy, I. M. *Nanotechnology* **2007**, *18*, 055102. (b) Nichkova, M.; Dosev, D.; Perron, R.; Gee, S. J.; Hammock, B. D.; Kennedy, I. M. *Anal. Biochem.* **2006**, *384*, 631−637.
(11) Kim, H. J.; Ahn, K. C.; Gonzalez-Techera, A.; Gonzalez-Sapienza, G. G.; Gee, S. J.; Hammock, B. D. *Anal. Biochem.* **2009**, *386*, 45−52.
(12) Franke, T.; Schmid, L.; Weitz, D. A.; Wixforth, A. *Lab Chip* **2009**, *9*, 2831−2835.
(13) (a) Rida, A.; Gijs, M. A. M. *Anal. Chem.* **2004**, *76*, 6239−6246. (b) Rida, A.; Gijs, M. A. M. *Appl. Phys. Lett.* **2004**, *85*, 4986−4988. (c) Luxton, R.; Badesha, J.; Kiely, J.; Hawkins, P. *Anal. Chem.* **2004**, *76*, 1715−1719.
(14) Cohen-Tannoudji, L.; Bertrand, E.; Baudry, J.; Robic, C.; Goubault, C.; Pellissier, M.; Johner, A.; Thalmann, F.; Lee, N. K.; Marques, C. M.; Bibette, J. *Phys. Rev. Lett.* **2008**, *100*, 108301.
(15) Derks, R. J. S.; Dietzel, A.; Wimberger-Friedl, R.; Prins, M. W. J. *Microfluid. Nanofluid.* **2007**, *3*, 141−149.
(16) Kang, T. G.; Hulsen, M. A.; Anderson, P. D.; den Toonder, J. M. J.; Meijer, H. E. H. *Phys. Rev. E* **2007**, *76*, 066303-1−066303-11.
(17) Krishnamurthy, S.; Yadav, A.; Phelan, P. E.; Calhoun, R.; Vuppu, A. K.; Garcia, A. A.; Hayes, M. A. *Microfluid. Nanofluid.* **2008**, *5*, 33−41.
(18) Lee, J.-T.; Abid, A.; Cheung, K. H.; Sudheendra, L.; Kennedy, I. M. *Microfluid. Nanofluid.* **2012**, 1−8.
(19) Biswal, S. L.; Gast, A. P. Rotational dynamics of semiflexible paramagnetic particle chains. *Phys. Rev. E* **2004**, *69*, 6448−6455.
(20) Melle, S.; Martin, J. E. *J. Chem. Phys.* **2003**, *118*, 9875−9881.
(21) Stenberg, M.; Nygren, H. *J. Immunol. Methods* **1988**, *113*, 3−15.
(22) Butler, J. E. *Methods-a Companion Methods Enzymol.* **2000**, *22*, 4−23.
(23) Kusnezow, W.; Syagailo, Y. V.; Ruffer, S.; Klenin, K.; Sebald, W.; Hoheisel, J. D.; Gauer, C.; Goychuk, I. *Proteomics* **2006**, *6*, 794−803.